

An experimental and modelling study of dual fuel aqueous ammonia and diesel combustion in a single cylinder compression ignition engine

Authors: James Frost^{a*}, Abdoulaye Tall^b, Abubakar Mahmud Sheriff^b, Dr Alessandro Schönborn^b, Dr Paul Hellier^a,

^a Department of Mechanical Engineering, University College London, London WC1E 6BT, U.K

^b World Maritime University, Fiskehamnsgatan 1, 201 24 Malmö, Sweden

***Corresponding author:** Department of Mechanical Engineering, University College London, London WC1E 6BT, U.K. Telephone +447858393022. Email: ucemjfr@ucl.ac.uk

Keywords: Ammonia Combustion, Compression Ignition, NO_x and Particle Emissions, Low-carbon fuel

Highlights

- **Ammonium hydroxide injected into the intake manifold contributed to engine load.**
- **Pilot injected diesel was required for initial ignition and flame propagation.**
- **Emissions of CO and particulates increased with ammonia injection.**
- **NO_x emissions appeared to form through both thermal and fuel-bound mechanisms.**
- **Significant unburnt ammonia was modelled at higher aspiration conditions.**

Abstract: The ability of ammonia to act as a hydrogen carrier, without the drawbacks of hydrogen gas (storage costs and low stability) renders it a potential solution to the decarbonisation of transport. This study combines both modelling and experimental techniques to determine the effect of varying the degree of aspiration of ammonium hydroxide (NH₄OH) solution, at different engine loads, in the combustion of a compression ignition engine. Ignition delay was extended as ammonia injection increased, causing an increase in peak in-cylinder temperature, but generally lower combustion quality; increasing incomplete combustion products, while decreasing particle size. The higher peak in-cylinder temperatures generally correlated with higher nitrous oxide (NO_x) emissions in the exhaust, though a fuel-bound nitrogen effect was apparent. Chemical kinetic modelling at equivalent conditions found increasing levels of unburnt ammonia with greater aspiration. Moreover, the ignitability of NH₄OH was found to improve in simulations substituting diesel with hydrogen peroxide direct injection.

1. Introduction

Electrification of the transport sector is rapidly progressing as emission regulations become more stringent and the industry converges on low carbon fuelled vehicles, however, there remains limitations; heavy duty machinery- such as HGVs and shipping vessels- continues to require diesel fuelled power units, in particular for the torque potential from these engines that operate at high compression ratios. For some sectors, such as maritime transport, the optimum solution may not be to electrify the sector, considering the range of autonomous operation, costs and the life-cycle impact of materials. Moreover, less developed countries will be slower to electrify as the necessary infrastructure is difficult to expand, and thus will likely continue to require more conventional ICEs as a primary means of transport. Continued ICE research and development- including the use of carbon-neutral feedstocks and more advanced after-treatment technologies- means that combustion technology is likely to remain in use for decades to come. Hydrogen has been touted as a potential solution¹ as an energy vector of electrical energy, but there are safety and cost concerns with storage,

making the growth of hydrogen infrastructure difficult. However, there exist alternatives to hydrogen refuelling. Tartakovsky and Sheintuch² provide an extensive review into the use of on-board steam reforming, which can utilise renewable feedstocks such as ethanol³ or methanol,⁴ partial oxidation of liquid petroleum gas,⁵ or exhaust gas recirculation,⁶ to produce hydrogen. This sees the benefits of hydrogen combustion i.e. no CO₂ is produced from the reaction of hydrogen and oxygen, but means that hydrogen refuelling itself is not required. However, this does not entirely alleviate safety issues of hydrogen, particularly its flammability, while the energy density of hydrogen is very low (10kJ/L) at ambient conditions. Ammonia is effectively a hydrogen carrier, with a hydrogen content of 17.8wt%,⁷ but is significantly more stable than hydrogen itself, although it possesses a higher toxicity that requires careful handling; between 150-300ppm is considered the maximum exposure.⁸ However, only moderate pressures and atmospheric temperatures are required to generate liquid-state ammonia, making transportation and storage much simpler relative to that of hydrogen.

Ammonia-fuelled combustion is not a new concept, having been used to fuel buses in Belgium in the 1940s due to a shortage of fossil fuels during the Second World War,⁹ and even in army vehicles by the US military in the 1960s.¹⁰ While this use of ammonia was employed in situations that necessitated the use of an alternative fuel due to unavailability of fossil fuel, it was a proof of concept that it was possible to run certain engines with an ammonia based fuel and this concept has received renewed interest in recent years given the need for low carbon renewable fuels.

Several studies in the 1960s investigated the fundamental reactions and flame characteristics of ammonia with various co-reactants¹¹; various stoichiometries of air, in H₂/O₂ and H₂/H₂O flames, as well as a pure oxygen environment, with Fenimore and Jones observing the reaction between NH₃ and NO as the dominant mechanism of ammonia consumption in H₂/O₂ flames; NO is initially produced from the oxidation of ammonia, potentially through 'attack of O atoms on ammonia'.¹² One subsequent study by Bian and Vandooren determined that hydroxyl radicals primarily consume NH₃ molecules to produce NH₂ radicals, which either react with H or OH radicals to form NH, and subsequently NO, or interact with NO directly to form diatomic nitrogen.¹³

The aforementioned studies primarily explored the fundamental mechanisms of ammonia combustion, and the resultant products, but others have looked into strategies to use ammonia in ICEs^{8,14,15,16,17}. Clear from these investigations is the need for a variety of techniques to enable stable ammonia combustion, with Starkman¹⁸ referencing the requirement of partially (25%) disassociated ammonia in the fuel feed- to yield a hydrogen level of at least 4-5wt%- to reach satisfactory performance (equivalent to 70% of the total engine load of hydrocarbon fuelled combustion). For some applications, it has been deemed non-feasible to use pure ammonia; the aforementioned spark ignition engines, tested in the 1960s with ammonia, can be operated with the pure ammonia, but the very high compression ratios required and poor ammonia combustion render this an unlikely solution for literal zero-carbon fuels.¹¹ In addition to raising the compression ratio in order to reduce the levels of unburnt ammonia in the exhaust, other strategies employed are H₂ doping, improved ignition systems and elevated engine load, though NO_x levels increase as a result of the latter.^{18,19} Additives are commonly employed in combustion experiments to enhance the ignition quality of a given fuel to bring it more in line with conventional fossil fuels and assist in drawing comparisons.²⁰ Nitrates and peroxides are commonly used but, in the case of ammonia combustion, hydrogen itself could be an attractive solution since it can be directly obtained from the ammonia utilised as the primary fuel.²¹ A catalyst can be used to decompose a proportion of the ammonia into pure hydrogen before entering the combustion chamber itself. Wang et. al utilised the exhaust gas as an oxygen source for the decomposition of ammonia over a ruthenium catalyst. However, despite the use of a catalyst, temperatures of 500°C were required, necessitating partial oxidation of the fuel to raise the temperature above that which the exhaust gas temperature of a diesel engine is normally able to reach. In addition, Comotti and Frigo²² utilised an ammonia cracking reactor to yield the possibility of

an SI engine to be run on a mixture of ammonia and hydrogen, in addition to the gasoline. However, high NO_x emissions were noted due to the high temperatures present in hydrogen fuelled combustion. Furthermore, the conversion of ammonia to hydrogen requires high temperatures and expensive catalysts, therefore research into using ammonia directly in energy applications, without the addition of hydrogen, has been considered.²¹

Blending of ammonia and gasoline could assist in the low combustion quality of the ammonia; the carbon-based fuel essentially acting as a promoter to allow the necessary temperatures and pressures to be reached for the ammonia to combust completely. Grannell et al.^{15,17} determined a blend of 70% ammonia and 30% gasoline to work well on a supercharged SI engine; the NH_3 emissions in the exhaust were proportional to the amount of ammonia in the fuel, while incomplete combustion products, CO and UHCs, increased as the proportion of gasoline was increased. It was also deemed essential that, for the after-treatment three-way catalyst to operate effectively, the fuel-air mixture should be maintained between stoichiometric and 0.2% rich, since lean operation was found to see over-oxidation of NH_3 and therefore a significant increase in NO and N_2O emissions. Furthermore, while NO_x emissions are prevalent, even in the absence of ammonia, levels of these emissions become much more sensitive to combustion stoichiometry where ammonia is present. Westlye et al.²³ measured NO, NO_2 , and N_2O emissions in a spark-ignition engine fuelled with ammonia, and reported that the amount of NO_2 formed was approximately 4% higher than under equivalent conditions with conventional gasoline used as fuel. The authors concluded that the increased amount of NO_2 produced during combustion was partly responsible for the formation of N_2O in the exhaust gases. The emissions of N_2O in the exhaust gas were below 60 ppm at all conditions tested, and were highest under the leanest conditions within a range of fuel-to-air equivalence ratios of 0.5-1.0 tested. A study by Ryu et al.²⁴ however, noted the requirement for 'substantial' gasoline injection, even at idle speed, for ammonia to combust, with increased ammonia injection duration and advanced injection timing contributing to further power output. As the amount of gasoline injected was increased, the contribution to power output from the ammonia decreased. Moreover, while increased ammonia injection lowered peak pressures due to lower flame speed and temperature, NO_x formation increased- suggesting that a portion of this NO_x was formed directly from the fuel- as did the ammonia slip, caused by traces of ammonia remaining unburnt. Emissions of both NO_x and ammonia were found to decrease at higher engine loads, suggesting preferential use of ammonia as greater power is demanded. Koike et al.²⁵ investigated the cold-start operation of an SI engine, utilising ammonia fed into a reforming catalyst, and were able to reduce NH_3 emissions to virtually zero; release of NH_3 is noted to be a major problem during cold-starts, as the exhaust gas needs to reach the necessary temperature for ammonia to react.

Compression ignition combustion is a promising method of ammonia utilisation, given the ability to potentially overcome the high resistance to autoignition exhibited by ammonia, using higher compression ratios than that of spark ignition engines. However, Dimitriou and Javaid reference that these ratios needed to be reaching 35:1 to 100:1, hence the interest of ammonia in marine applications,²⁶ while Reiter⁸ notes that ammonia is only combusted successfully if introduced in the air intake system and diesel is injected to provide the ignition energy; controlled autoignition of ammonia only was found not to be possible, even at a 30:1 compression ratio. Several studies^{20,27-29} have used homogenous charge compression ignition (HCCI) combustion with a variety of fuels based on the high compression ratios and low combustion temperatures (for low NO_x output) exhibited, such that an almost limitless number of fuels could be tested. However, compression ignition engines are a more realistic application of ammonia-derived fuels, and numerous investigations have looked into a range of techniques.²⁶ Boretti³⁰ was able to simulate diesel and NH_3 direct injection, noting that power efficiencies approaching those of pure diesel could be achieved. Lamas and Rodriguez³¹ also investigated ammonia and diesel direct injection in a numerical study that proposed ammonia as a

way of reducing the high NO_x emissions produced when pure hydrogen is used. Gill et. al conducted a study into the use of ammonia, dissociated ammonia and hydrogen as energy contributors to diesel led combustion, observing a 15% decrease in CO₂ emissions when substituting 3% of the intake air with NH₃.³²

A common theme in literature is the suggested use of blends of ammonia, either with other hydrogen derived fuels or in combination with a small amount of fossil fuel, acting as pilot injected ignition and combustion promoters. To this end, this study presents testing of pilot ignited aqueous ammonia in a light duty diesel engine in order to provide insights into its feasibility as a sustainable fuel for combustion engines, potentially in the heavy duty and marine sectors.

The study by Reiter and Kong provided a comprehensive study of compression ignition engine operation using both diesel and ammonia.⁸ However, ammonia itself is difficult and dangerous to handle and so, for the current study, a solution of ammonium hydroxide (NH₄OH) was instead used to investigate the potential contribution to energy release during combustion when ammonia is present in this form. Ammonium hydroxide is synthesised by saturating water with ammonia, and could be a simple way of utilising ammonia within combustion engines (providing the water does not inhibit any combustion or result in excessively high pollutants) without the need for compression or cooling of ammonia itself. However, the injection of ammonium hydroxide can be expected to alter emissions characteristics beyond that which can be accounted for by the ammonia itself. This is, to the best of our knowledge, the first attempt of using this form of ammonia in an internal combustion engine. A series of experiments were undertaken in a single cylinder diesel engine investigating combustion and emissions characteristics where a range of engine loads were achieved by varying the relative proportion of intake air aspirated ammonium hydroxide solution and direct injected fossil diesel fuel.

2. Material and Methods

2.1. *Experimental Methods*

2.1.1. Research Engine

The research engine, specified in Table 2.1 below, was a direct-injection, custom built, 4-stroke single cylinder compression-ignition engine. The majority of components (cylinder head, intake manifold, fuel injector, piston and connecting rod) were from a 2.0 litre turbocharged diesel engine (Ford Duratorq CD132 130PS). For the engine crank case, a Ricardo Hydra single cylinder crank case was employed; an adaptor plate was required to utilise the head in the single cylinder configuration. A David McClure DC motor dynamometer, capable of motoring the engine up to 5000 rpm, was controlled by a Cussons test-bed console, with further details of the research facility published previously.³³ The combustion chamber itself, as stated in Table 2.1, consisted of a ω shaped bowl piston and a flat roof with two intake and two exhaust valves, and a centrally located injector.

Table 2.1: Diesel Engine Specifications

Engine Head Model	Ford Duratorq
Engine Crankcase Model	Ricardo Hydra
No. of Cylinders	1
Cylinder Bore (mm)	86
Cylinder Stroke (mm)	86
Swept Volume (cm³)	499.56

Geometric Compression Ratio	18.3 : 1
Max In-Cylinder Pressure (bar)	150
Piston Bowl Design	Central ω bowl
Fuel Injection Pump	Delphi single-cam radial-piston pump
High-pressure Common Rail	Delphi solenoid controlled (Max 1600 bar)
Diesel Fuel Injector	6-hole solenoid valve injector (Delphi DFI 1.3)
Fuel Injection System	1 μ s duration (EMTRONIX EC-GEN 500)
Crank Shaft Encoder	1800 ppr (0.2 CAD resolution)

2.1.2. Exhaust emissions measurement

Gaseous emissions (CO , CO_2 , and NO_x) were all measured using a Horiba MEXA 9100H EGR automotive gas analyser, sampling the engine exhaust approximately 400 mm downstream of the exhaust valves. Within this instrument, a non-dispersive infrared (IR) adsorption analyser determined the concentration of CO and CO_2 , while NO_x emissions were obtained using a chemiluminescent analyser. Particulate emissions (size distribution, mass and number) were measured using a particulate spectrometer (Cambustion DMS500). The heated line connecting the engine exhaust to the gas analyser was heated to 190°C to prevent condensation of gaseous species in the exhaust.

2.1.3. Dual fuel injection set-up

In order to reduce any potential reactions, or indeed phase separation, between NH_4OH and diesel, mixing of the two fuels and subsequent injection through the same injector was deemed undesirable. Further, the Delphi injector used for diesel injection was not compatible with ammonium hydroxide due to its very poor lubricity, while the constant evaporation of ammonia into the gaseous phase may have caused injection problems. Therefore, a system using a pilot direct injection of diesel was employed alongside aspiration of the ammonium solution. The fossil diesel utilised was of zero FAME content and obtained from Haltermann Carless, while the 28% NH_3 Ammonium hydroxide solution was sourced from Sigma-Aldrich (boiling point: 38°C , melting point: -58°C , density: 0.9g/ml at 25°C , vapour pressure: 2160mm Hg at 25°C).

For all engine experiments, ammonium hydroxide was aspirated into the engine air intake manifold via a port fuel injector, while the fossil diesel fuel was direct injected and supplied by a conventional common rail circuit. Given the constant evaporation of ammonia from this solution, however, it was important to minimise the potential escape of ammonia via an open lid. A pressure vessel containing the ammonium solution was pressurised to 2 bar and connected via a short length of pipe to a Bosch gasoline fuel injector installed into the air intake of the diesel engine. Initial attempts were made to blend a fuel with a high cetane number, diethyl ether (DEE), with the aqueous ammonia in an attempt to achieve autoignition of the ammonia in the absence of pilot ignition. This, however, did not achieve ammonia combustion as it was noted that DEE and ammonium hydroxide were not miscible.

Therefore, for all experiments reported in this work, fossil diesel was direct injected at a constant injection timing of 10 degrees BTDC and 550 bar injection pressure, so as to reach in-cylinder conditions at which the intake air aspirated aqueous ammonia contributed to heat release during combustion. Table 2.2 summarises the conditions of the pilot ignited ammonium hydroxide engine tests. Diesel and aqueous ammonia injection durations during each test are outlined in Table 2.2, while the engine speed was maintained at 1200rpm for all tests.

Initially, during diesel-only combustion, engine load was maintained at the desired value by adjusting diesel injection durations on the fly. Ammonium hydroxide was then aspirated into the engine in order to increase the engine load by 0.5 bar and 1 bar, during which time the diesel injection duration was maintained at the rate that corresponded with contributing 4 bar IMEP (645 μ s). Diesel injection was then lowered at maximum load (D4A1: 5bar IMEP), where ammonium hydroxide was contributing to 20% of the energy contribution, and the ammonium hydroxide aspiration rate was held constant as the overall engine load was lowered (a 2750 μ s injection duration). This thereby increased the proportion of energy released by the aqueous ammonia, relative to diesel (A1D3.5: 22% NH₄OH energy contribution, A1D3: 25% NH₄OH energy contribution).

Both the frequency and duration of opening of the PFI injector supplying aqueous ammonia could be controlled but, for ease of comparison, only the duration was altered, while the frequency was kept to a low value of 1.9Hz. Injector calibration was performed by bench testing the injection set-up, using water rather than NH₄OH due to similar physical properties, but greater hazard, of handling ammonium hydroxide (full face masks were used when ammonium hydroxide was exposed to the atmosphere). A fixed injection frequency and varying durations were output from the injector driver and measured using an oscilloscope, timed for 1 minute, and the quantity of water remaining in the vessel subtracted from the original volume. This enabled flow rates to be calculated for a given injector pulse duration.

Initial tests were performed with injection of fossil diesel only, with the injector opening duration set so as to maintain a constant engine IMEP of 4 bar, 4.5 bar and 5 bar. In following experiments, the level of ammonium hydroxide aspirated into the intake manifold was gradually increased so as to increase the engine IMEP by 0.5 bar and then 1 bar (4.5 bar and then 5 bar overall respectively). Subsequently, the amount of diesel injected was gradually reduced, while maintaining a constant level of ammonium hydroxide aspiration, such that the engine load was reduced to 4.5 bar and then 4 bar IMEP. This was to allow a comparison to be made between combustion at equivalent engine loads, but with differing energy contributions from the aqueous ammonia and fossil diesel.

Table 2.2: Overview of Test Conditions

Test	Diesel Injection (us)	Ammonia Injection (us)	Inlet Temperature (°C)	Diesel Load (bar IMEP)	Ammonia Load (bar IMEP)	Ammonia Load Contribution (%)	Abbreviation
1	662	0	83.1	4	0	0	<i>D4 (Start)</i>
2	692	0	83.8	4.5	0	0	<i>D4.5</i>
3	730	0	84.1	5	0	0	<i>D5</i>
4	645	1400	74.8	4	0.5	11	<i>D4A0.5</i>
5	645	2750	36.1	4	1	20	<i>D4A1</i>
6	611	2750	28.5	3.5	1	22	<i>A1D3.5</i>
7	582	2750	27.3	3	1	25	<i>A1D3</i>
8	639	0	28.0	4	0	0	<i>D4(ST)</i>
9	643	0	83.1	4	0	0	<i>D4(End)</i>

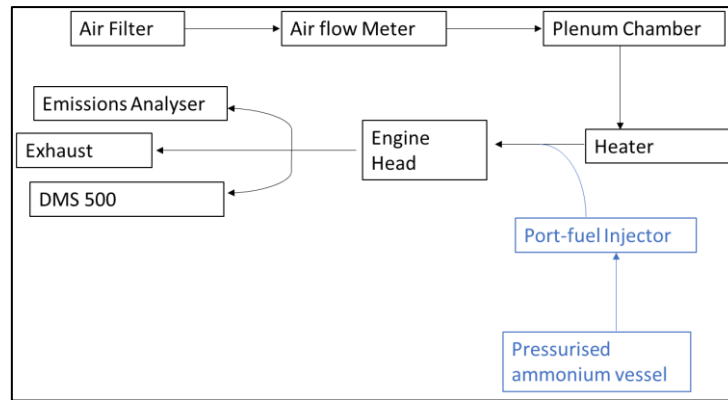


Figure 2.1: Schematic of air intake system

Intake air temperatures were raised utilising an inline air heater (Secomak 571), placed approximately 260mm prior to the port injector, and 330mm upstream of the intake manifold. The temperature was set to 80°C using a PID control system, though the actual inlet temperature, as indicated in Table 2.2, varied depending on the injection rate of ammonium hydroxide. As seen from Figure 2.1, port fuel injection was placed downstream of the heater, to remove any risk of accidental ammonia ignition in the intake. It was noted though that, due to ammonium hydroxide injection, the air temperature reduced to atmospheric levels once it had reached the manifold, necessitating the diesel test D4(ST), that utilised pure diesel combustion at the same air intake temperatures. Ammonium hydroxide port fuel injection was achieved using a Hartridge (HK852) signal unit to send a signal of set frequency and duration that released ammonium solution into the intake manifold at a pressure of 2 bar. It was assumed that chemical interaction between ammonium hydroxide and lubricant oil was negligible, due to high turnover rate and relatively low concentration of ammonium hydroxide present in the air manifold.

2.2. Modelling Methods

The ignition of diesel fuel and ammonia in air is dominated by the chemical reaction kinetics of the two fuels interacting with air at the stoichiometries, temperatures and pressures encountered throughout the diesel engine cycle. In order to understand and analyse the chemical kinetics of the ignition trends, an effort was made to model the engine experiments, using zero-dimensional chemical kinetic reactor models, that could model the fuel and air stoichiometries in a simplified way.

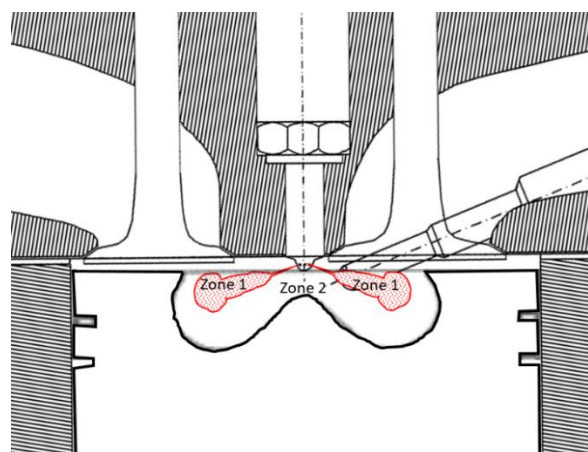


Figure 2.2. Engine reactor model showing Zone 1 (ignition zone) and Zone 2 (main zone)

It was assumed that the engine consisted of two reaction zones: Zone 1 consisted of the reaction zone around the diesel fuel spray, in which initially a mixture of evaporated aqueous ammonia and air were present, and into which the diesel fuel was injected and ignited. Zone 2 comprised the remaining combustion chamber, containing either air or a mixture of evaporated aqueous ammonia and air. Zone 2 did not receive any diesel fuel injection, but its pressure and temperature were affected by the ignition taking place in zone 1. The pressure in Zones 1 and 2 was assumed to be equal. Zone 1 was assumed to be entirely immersed within Zone 2, which is why heat transfer to the walls took place between Zone 2 and the walls, and heat transfer from Zone 1 only took place to Zone 2.

During the time in which the inlet and exhaust valves are closed, the only mass entering the control volume is that of the pilot fuel injected into Zone 1. The energy balance for each of the two zones is described by the first law of thermodynamics (equation 1):

$$\frac{dU}{dt} = \frac{dQ}{dt} - \frac{dW}{dt} + \frac{dm_i}{dt} \dot{h}_i \quad \text{equation 1}$$

where Q is the amount of heat entering the control volume, W is the amount of work done by the control volume, and m_i and h_i are the mass and enthalpy of the injected pilot fuel, respectively. In the case of Zone 2, m_i is equal to zero.

The heat transfer from a reactor zone was calculated using the semi-empirical model of Woschni³⁴ for a four-stroke four-valve quiescent Diesel engine using equation 2:

$$h_c = 3.26 B^{-0.2} p^{0.8} T^{-0.55} s \quad \text{equation 2}$$

where h_c is the heat transfer coefficient, B is the cylinder bore, p is the cylinder pressure, T is the global zone temperature, and s is taken as the instantaneous piston velocity.

The instantaneous piston speed s was calculated using equation 3:

$$s = \frac{c}{2} \cdot 2\pi \cdot f \cdot \sin(\theta) \quad \text{equation 3}$$

where c is the piston stroke, f is the rotational frequency, and θ is the cycle crank-angle.

The cylinder volume was calculated using equation 4:

$$v = v_{clear} + c - a \cdot \cos(\theta) + \sqrt{l^2 - (a^2(\sin^2(\theta)))} \quad \text{equation 4}$$

The work done by the control volume was calculated using equation 5:

$$\frac{dW}{dt} = p \frac{dv}{dt} \quad \text{equation 5}$$

The cylinder pressure p is calculated using the ideal gas equation 6:

$$p = \frac{NRT}{v} \quad \text{equation 6}$$

where N is the number of total number of moles in the cylinder, and R is the universal gas constant $R=8.314 \text{ J/K}\cdot\text{mol}$.

The total number of moles and their temperature varies according to the chemical kinetic modelling of the combustion mechanism. The chemical reactions were modelled using a previously published chemical kinetic mechanism³⁵, with n-dodecane ($C_{12}H_{26}$) as a surrogate for the reference diesel utilised in the engine experiments.

Gas exchange was assumed to take place during inlet and exhaust valve opening only, between both zones and the intake and exhaust manifolds-in order to model the appropriate gas compositions for the engine cycle. The reactor models were coded using the Python 3.7 programming language and using the Cantera 2.4.0 software module.³⁶

3. Results and Discussion

3.1. Ignition Delay

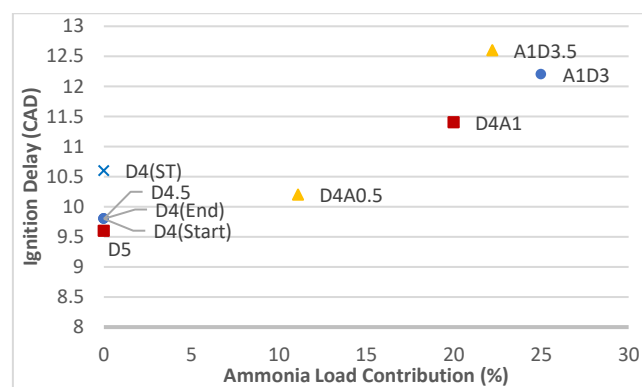


Figure 3.1: Ignition delay during Diesel-led combustion at varying engine loads and ammonia contributions. Blue circle (4bar), Yellow triangle (4.5bar), Red square (5bar)

Figure 3.1 shows the observed ignition delay at each of the fuel and load combinations tested (Table 2.2), where the duration of ignition delay is defined as the interval in CAD between the start of the diesel fuel injection (based on injection timing of the Emtronix EC-GEN-500 software) and the start of combustion (defined as the first instance at which net heat release becomes positive). Immediately apparent from Figure 3.1 is a significant increase in the duration of ignition delay as more of the engine load is attributed to the combustion of ammonia, both at constant engine load and where the diesel fuel injection duration was held constant. One of the most notable features of the aspiration of aqueous ammonia was its effect on the intake air temperature; the intake temperature for all tests was set at 80°C (except for the D4(ST) test), however the ammonium hydroxide injection occurred downstream of the heater and the evaporation of this solution lowered the intake air to almost room temperature just prior to the engine intake valves. This reduced intake- and thus compression- temperature would naturally see a decrease in the rates of the early stage combustion kinetics, which dictate the ignition delay period, and have a knock-on effect on the combustion conditions itself. Since this reduction in the intake temperature was noted during all tests with aspirated aqueous ammonia, and would therefore obscure any notable effect on the ignition delay period attributable to the ammonia itself, a test was also performed at 4 bar IMEP for diesel only with no heating of the air intake (D4(ST) test). As illustrated in Figure 3.1, with reduced intake air temperature the ignition delay increased from 9.8 (D4(Start)) to 10.6 (D4(ST)) for the diesel only tests at constant load. While this indicates that a significant proportion of the ignition quality of the air fuel mixture may be due to the temperature of the intake air, this delay period is still less than that of the

ammonia and diesel test conducted at the same load condition (A1D3). As noted extensively in the literature, ammonia possesses high resistance to autoignition- the autoignition temperature of ammonia is 651°C compared to 225°C for diesel²⁴- far greater than that of other hydrogen carrier fuels such as methanol or diatomic hydrogen, and so it is likely that the extended ignition delay of diesel-ammonia combustion is attributable to the ammonia itself. It is also interesting to note that the ignition delay variability seen in Figure 3.1 is minimal when comparing engine load changes for the same fuel, for example the ignition delay of diesel only combustion varies from 9.8 CAD to 9.6 CAD at 4 bar to 5 bar IMEP respectively, which can likely be attributed to the higher in cylinder temperatures at the higher load condition.

A multiple linear regression analysis of the data was carried out in an attempt to identify the relative effects of engine load fraction attributed to the diesel fuel load fraction (d), and total combined engine load (t) on the duration of ignition delay (τ). The equation found for the multiple linear regression analysis for this relationship is given in equation 7 below:

$$\tau = 21.16 - 10.37 \cdot d - 0.255 \cdot t \quad \text{equation 7}$$

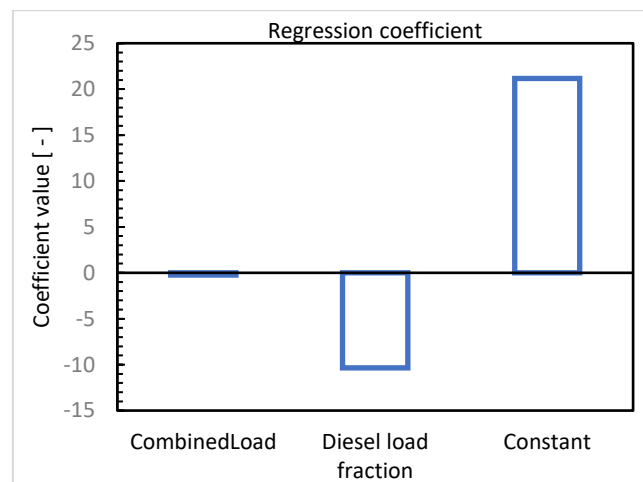


Figure 3.1. Magnitude of correlation coefficient of various effects on ignition delay

Figure 3.2 shows the magnitude of the correlation coefficients found in the regression analysis of engine load and fuel contribution effect on ignition delay. Immediately apparent in Figure 3.2 is the significantly greater impact of diesel load fraction relative to the combined engine load, confirming the trends apparent in Figure 3.1.

An initial study by Gray confirmed that combustion of ammonia through means of compression alone was not feasible given the compression ratios and elevated inlet temperatures required for only moderate performance.¹⁰ The notable reduction in temperature of the inlet air is due to the water in the ammonia solution used. Pure ammonia is a toxic gas and thus carries a considerable safety risk. This toxicity also means that care needs to be taken to avoid ammonia slip, whereby ammonia enters the atmosphere with other pollutants via the engine exhaust; catalysts may be used in this case, and since these are already present in modern powertrains for road transport, it may not add considerable cost. The use of ammonium hydroxide solution may mitigate some of these toxic effects, however, the use of this ammonia source has been shown here to have a negative impact on the ignition quality of the direct injected diesel fuel, attributable to the very high heat capacity and dilution of the reacting mixture, and potentially limiting the contribution to engine IMEP. It is apparent, however, that the air

intake temperature is not the only reason behind the change in ignition delay- the high resistance of ammonia to autoignition is clear.

3.2. Heat Release Rate

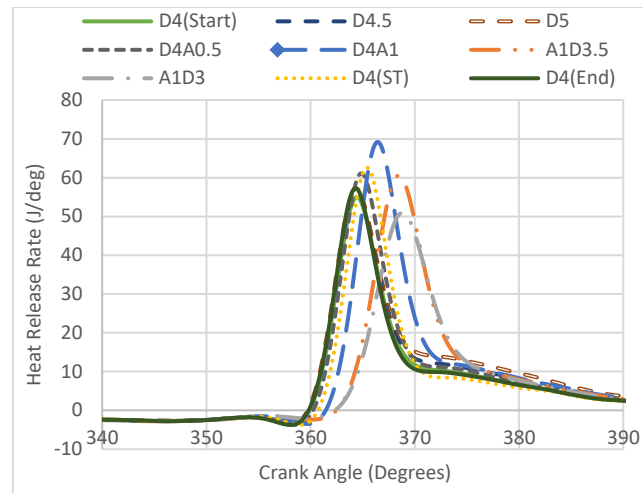


Figure 3.3: Apparent net heat release rate during co-combustion of diesel fuel and aspirated aqueous ammonia at varying engine IMEP

The heat release rates shown in Figure 3.3 indicate that combustion phasing was retarded as a greater proportion of ammonia was responsible for energy release. Initially, it can be seen that a change in the engine load from 4 to 5 bar IMEP when using diesel only saw little change in combustion phasing (from D4(Start) to D4.5 to D5); the peak heat release rate (pHRR) is generally dictated by the ignition delay period, which was similar for all 3 engine loads, while a slight difference was noted in the diffusion controlled combustion phase. This is expected since more energy is released at higher loads and limited energy increase is attributable to the premixed combustion phase given that the ignition delay period (and therefore the amount of fuel and air mixed prior to the start of combustion) is very similar in these cases.

It can also be seen in Figure 3.3 that, from the difference between D4(Start) and D4(End), the engine drift from the start of the day to the end was minimal in terms of heat release, while the delayed phasing of the D4(ST) test condition also highlights the effect of operating the air intake at atmospheric conditions. In general, ignition delay and heat release rate can be expected to reduce and increase slightly from the start to end of a testing day, due to higher oil and coolant temperatures and better lubrication of the injector through sustained use of diesel. The fact that this potential engine drift is not apparent here gives more certainty towards the impact gauged from ammonium hydroxide aspiration. The cooler inlet air reduces reaction rates and thus extends the ignition delay period, leading to higher peak heat release. Comparing the heat release rates of D4(ST) and A1D3, it is apparent that the addition of ammonia delayed the start of combustion considerably; in general, a longer delay period sees a higher peak heat release rate but it can be seen that the substitution of diesel fuel for energy release from aqueous ammonia resulted in an appreciable decrease in the values of peak heat release. In the case of A1D3, energy release occurs later into the expansion stroke at higher volume conditions and this likely results in greater heat losses due to the larger exposed surface area of in-cylinder wall. This retardation was very pronounced, and resulted in a lower combustion stability that can be observed from the large coefficient of variation (COV) of engine loads calculated

for this test, as shown in Table 3.1 below. Indicated by the COV values is an increase in combustion instability with an increasing ammonium load contribution and decrease in overall engine load.

Table 3.1: Coefficient of variation (%) of base diesel tests at varying loads, compared to tests conducted using 0.5bar and 1bar ammonium load contribution

Test	COV (of IMEP) (%)
D4 (Start)	1.05
D4.5	0.84
D5	0.74
D4(ST)	0.97
D4 (End)	0.94
D4A0.5	1.10
D4A1	0.96
A1D3.5	1.15
A1D3	1.55

Figure 3.3 also shows heat release rates at 4.5bar IMEP and at 3 different conditions; with diesel only (D4.5), diesel contributing 4bar IMEP and aspirated aqueous ammonia 0.5bar (D4A0.5), and when aqueous ammonia is contributing 1 bar and diesel 3.5bar (A1D3.5). Apparent from the heat release at this condition is that when increasing the amount of aspirated aqueous ammonia from zero to a contribution of 0.5 bar IMEP, the ignition delay and the peak rate of heat release rate both increase. As the contribution of ammonia was further increased to 1 bar IMEP, the ignition delay increased, but the peak rate of heat release began to decrease. This suggests that there was sufficient diesel injection in the D4A0.5 test to maintain reaction rates such that the dual fuel charge ignited without extending the delay period significantly relative to diesel only combustion. As a result, the peak heat release rate increases in line with the longer delay period in the case of the D4A0.5 test. In addition to greater heat losses, the lower peak heat release rate of the A1D3.5 can likely be attributed to the extended duration of ignition delay resulting in an over-dilution of the diesel fuel in air. Similar observations have been made in Reactivity Controlled Compression Ignition (RCCI) experiments employing methanol, another premixed fuel with low ignition quality, in combination with diesel fuel.³⁷

5 bar IMEP conditions, with and without the use of ammonia, are outlined. In this case, the load appears to be high enough that in-cylinder conditions are suitable for ammonia to contribute effectively towards energy release (compared to when the total load is set to 4bar IMEP, with ammonia also contributing 1 bar). The delay period is extended in the D4A1 test, and therefore a higher pHRR is observed compared to the D5 test, as a result of the longer period allowed for premixing of fuel and air. A further observation is that, when the engine load is increased using ammonia, the difference is observed primarily in the premixed phase. When comparing pure diesel combustion at 5 bar (D5), and combustion at 5 bar utilising 1 bar IMEP from ammonia, the premixed burn fraction was increased, from approximately 56% to 63%. Furthermore, increased ammonia combustion contribution saw the extent of the premixed fraction extend further to 67% for the A1D3.5 run and 65% for the A1D3 test. Naturally a greater proportion of the diesel is combusted in the premixed phase due to the longer delay period, but it is suggested that ammonia combustion is also more prevalent in the premixed phase.

3.3. CO emissions

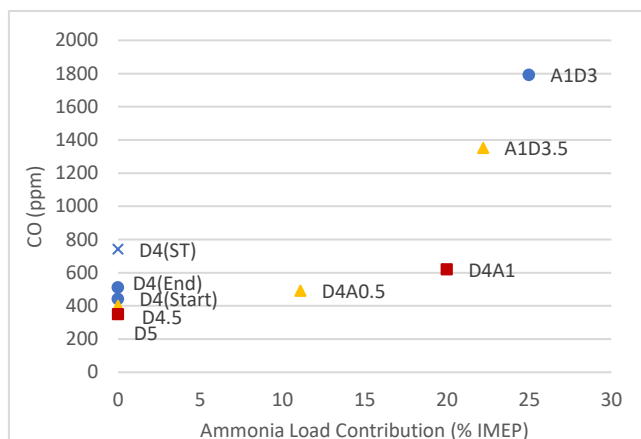


Figure 3.4: Carbon monoxide concentrations in the exhaust gas at various engine loads and ammonia injection rates. Blue circle (4bar), Yellow triangle (4.5bar), Red square (5bar)

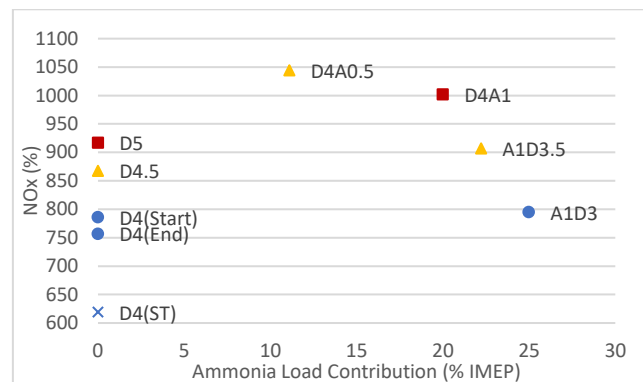
Figure 3.4 shows that, for all engine loads, as the amount of aqueous ammonia supplied was increased- with a concurrent reduction in the duration of the diesel injection- levels of CO in the exhaust increased. This is contrary to the study of Grannell et al. with gaseous ammonia in an SI engine, where an increased proportion of fossil fuel seeing higher CO emissions¹⁷. While the study by Reiter of CI combustion of ammonia and diesel/biodiesel did not measure CO emissions, a similar trend in HC emissions to the one seen here in CO concentration was noted, and postulated to be due to lower combustion temperatures.⁸

A further related explanation is that the extended ignition delay period observed with increasing proportions of aqueous ammonia present, potentially increased fuel impingement on the cylinder walls and thus levels of incomplete combustion. When the duration of diesel injection is reduced, temperatures are lowered further and, eventually, saw unstable combustion in the case of the A1D3 test, indicated by the highest COV in IMEP shown in Table 3.1. Considering the diesel only experiments, CO levels reduce at higher loads, primarily as a result of higher combustion temperatures, rather than the trend noted in SI combustion¹⁷ whereby the CO output is far more sensitive to the actual amount of fuel carbon injected (with dissociation also likely an important factor in CO formation and typically absent during CI combustion). While, in the case of the diesel only tests, higher engine loads see a decrease in CO emissions, the same trend is not apparent where higher levels of aspirated aqueous ammonia were used to increase the power output (Figure 3.4), suggesting that the resultant reduction of in-cylinder temperature dominates the CO emissions and produces an apparent reduction in diesel fuel combustion efficiency.

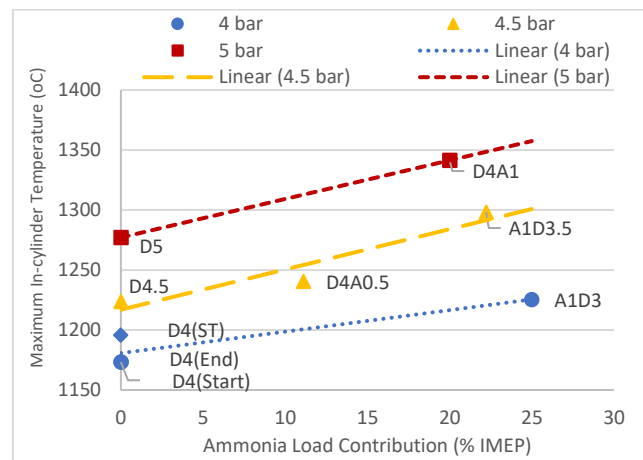
One potential contributor to the increased CO emissions with increasing presence of aqueous ammonia is the reduced intake air temperature caused by the increase in heat capacity of the charge gas that the ammonium hydroxide affords; not only does this lead to the aforementioned extended ignition delay through reduced reaction rates it will likely also impair the efficiency of fuel air mixing, which could see an increase of overly lean or rich regions within the combustion zone, and therefore greater CO formation. However, as can be seen from the D4(ST) result in Figure 3.4 with an intake air temperature of 25°C, this reduced temperature sees only a 0.03% increase in CO emissions compared to D4(Start) and D4(End), as opposed to the 0.14% increase with aspiration of aqueous ammonia at the same load of 4 bar IMEP (A1D3). This observation suggests that a decreased inlet air temperature alone is not sufficient to explain the observed increase in CO concentration. Furthermore, there

appears to be a linear increase in CO emissions when reducing the duration of diesel injection from 645 μ s to 582 μ s (D4A1 to A1D3), which is a more considerable increase than seen when gradually adding ammonia to a fixed quantity of diesel. It may be inferred from this, again, that a minimum engine load, or duration of diesel injection, is required for the aspirated ammonia to contribute effectively to the combustion process and energy release. It is suggested that when the duration of diesel injection is too low, combustion does not propagate effectively through the premixed aqueous ammonia and the combustion efficiency of the direct injected diesel, resulting in significantly elevated levels of CO in the exhaust (Figure 3.4).

3.4. NO_x emissions



(a)



(b)

Figure 3.5: (a) NO_x concentrations in the exhaust gas at various engine loads and ammonia injection rates. Blue circle (4bar), Yellow triangle (4.5bar), Red square (5bar) and (b) peak in-cylinder global temperatures calculated at various engine loads and ammonia injection rates. Blue circle (4bar), Yellow triangle (4.5bar), Red square (5bar)

The aforementioned higher temperatures at higher engine load can also be inferred from Figure 3.5a with an increase in NO_x emissions at higher load conditions with the use of diesel alone, while the calculated maximum global in-cylinder temperatures shown in Figure 3.5b further support this assumption. Maximum in-cylinder temperatures were calculated assuming the ideal gas law applies; it is assumed that the molar flow into the cylinder is constant, therefore the molar flow of ammonium

hydroxide replaces the same moles of air, thus changing the mass. The new mass flow rate of air, with the addition of the mass flow of ammonium hydroxide, sees an overall reduction in mass flow rate relative to charge gas comprising air alone. An increase in temperature and NO_x with engine load are to be expected given the longer fuel injection with increasing load and thus higher combustion temperatures where rates of NO_x formation are highly temperature dependent.³⁸ Figure 3.5a shows an initial increase in NO_x levels with the aspiration of aqueous ammonia, relative to the diesel only test at the same engine load. This is in line with maximum in-cylinder temperature, illustrated in Figure 3.5b, though the small temperature increase alone observed in the D4A0.5 test, relative to D4.5, is unlikely to explain the large increase in NO_x emissions of just under 200ppm. In the case of the D4A0.5 test, the slightly longer ignition delay period (Figure 3.1) and higher pHRR (Figure 3.3) relative to diesel only at the same load, would likely cause the slightly higher in-cylinder temperatures. However, it is postulated that, in the case of ammonia combustion, NO_x is influenced by nitrogen in the ammonia when there is no appreciable change in maximum temperature, as is the case when comparing the tests at 4.5 bar IMEP with 0 and 12 % load contribution from the aspirated ammonia, D4.5 and D4A0.5 respectively. Moreover, it is suggested that the calculated global temperatures (which assume ideal gas behaviour of the cylinder contents) are inherently unlikely to show complete correlation with NO_x given that locally hotter regions are not discernible. This is addressed further in Section 3.6, in which for a subset of the experimental conditions reaction kinetics and temperatures during combustion are simulated utilising a two-zone model. In the case of the D4A0.5 test, NO_x levels are higher than in diesel only combustion at 5 bar (Figure 3.5a), D5, despite a significantly lower maximum in-cylinder temperature (Figure 3.5b). This indicates an effect beyond maximum global temperature in explaining NO_x emissions during diesel and aspirated ammonia combustion. There is some potential that the nitrogen content of the aspirated ammonia itself contributes to NO_x formation. Wang and Herreros²¹ noted that an increase in ammonia increased NO_x levels during experiments in a diesel engine, and the ratio of NO_2 to NO also increased. Reiter, however, observed relatively low levels of NO_x emissions with the use of ammonia at levels of energy displacement up to 60% (after which the influence of fuel-bound nitrogen in the NH_3 molecule becomes prevalent), as a result of the lower combustion temperatures when NH_3 is aspirated.⁸ Ryu,²⁴ meanwhile, observed an increase in NO_x with combustion of ammonia in an SI engine, attributed to the presence of fuel bound nitrogen. Grannell also noted a contribution of fuel-bound nitrogen, but highlighted the lowering of adiabatic flame temperature that ammonia affords as the main driver of trends in NO_x emissions during combustion.¹⁷ Furthermore, Duynslaegher stated that, when using ammonia in an SI engine, the 'nitrogen monoxide concentration was very low due to relatively low combustion temperatures', implying little impact of nitrogen in the ammonia molecule on the type of nitrogen emissions in the exhaust.¹¹

The influence that the ammonium solution aspiration has on the stoichiometry of the combustion mixture may also play a role in explaining the discrepancy in NO_x levels and peak in-cylinder temperature. While diesel combustion occurs predominately at stoichiometric conditions, ammonia combustion will occur at more lean conditions, having been delivered to the combustion chamber as a homogeneous mixture with the intake air. Reiter and Kong observed that, with a diesel energy contribution of greater than 60%, the BSFC of ammonia increases substantially, suggesting this could be due to the injected ammonia burning under conditions that were 'too lean' when concentrations were too low.⁸ As stated previously, the D4A0.5 test- with only 12% of engine load attributable to the aspirated ammonia- produced slightly higher NO_x than the D4A1 test at higher 5 bar IMEP and ammonia providing 20 % of the engine load. This may be inferred as an indication of a peak level of ammonia injection in exacerbating NO_x emissions; ammonia levels are sufficient for appreciable NO_x formation from the fuel bound nitrogen, but any decrease in temperature arising from a decrease in stoichiometric diesel combustion and increase in lean premixed ammonia combustion is insufficient to reduce thermal NO_x (but this is the case when ammonia contributes greater than 20% of the total

load). This could potentially explain why the maximum temperature observed in the D4A0.5 test was less than 20°C higher than that of pure diesel and over 50°C when ammonia contributed 1bar out of 4.5bar IMEP; ammonia was overdiluted at the lower injection rate. Moreover, a study by Talibi et. al, utilising pure hydrogen in tandem with pilot injected diesel, showed that NO_x levels varied markedly- especially at earlier phases of combustion- depending on whether a sample was taken within the diesel spray or in between sprays. Within a spray the absence of air likely resulted in lower burn rates, while the hydrogen concentration was low. Between sprays, where hydrogen and diesel were mixed more homogeneously, the high flame temperature of hydrogen in addition to heat release from diesel combustion was reflected in higher NO_x. Also observed was a threshold of hydrogen energy contribution, after which flame temperatures exceeded the amount required for NO_x formation, but below which the hydrogen-air mixture was overlean and elevated NO_x emissions relative to diesel only combustion were not observed.³⁹ It is again suggested that- in the current study- despite a slight decrease in maximum global temperature, the D4A0.5 test was possibly an 'optimal' condition to run the engine at for stable combustion, with both thermal and fuel-bound NO_x prevalent.

It has been noted before, but at this point may be pertinent to mention again, that NO_x formation requires both high temperatures and sufficient time at these conditions. Figure 3.6 indicates the time of occurrence of both maximum in-cylinder temperatures and peak heat release rates, with the interval between these two events tentatively suggested to correlate with the duration of high temperature conditions. Comparing the tests at 4.5 bar IMEP, diesel only combustion (D4.5) sees pHRR occur at 364.4 CAD and the maximum temperature is observed at 380.4 CAD, while during the D4A0.5 run, with 12 % of the engine IMEP contributed by the aspirated aqueous ammonia, the pHRR is shifted slightly later to 364.8 CAD and the maximum temperature are seen slightly earlier, at 379.6 CAD. Furthermore, when the contribution of ammonia is increased further (A1D3.5) to 22 % of IMEP, the time of pHRR is retarded even further to 368.4 CAD, but the timing of maximum temperature was relatively unchanged, at 380 CAD. The shorter interval between peak heat release and maximum temperature when ammonia is injected at greater levels explains why the NO_x levels may not be directly linked to peak in-cylinder temperatures, as these temperatures are present for a shorter duration than diesel only combustion.

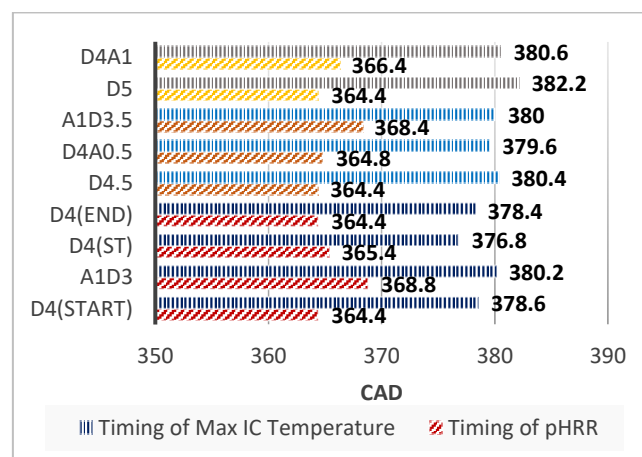
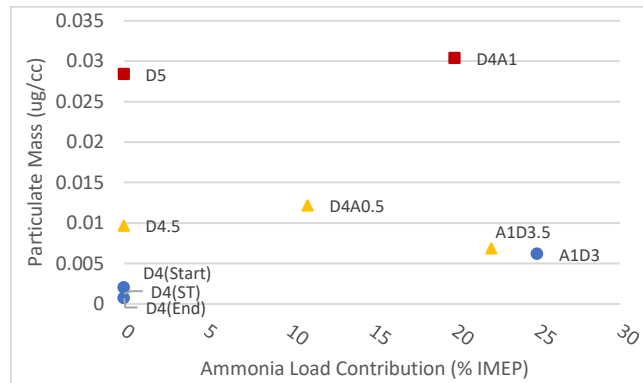
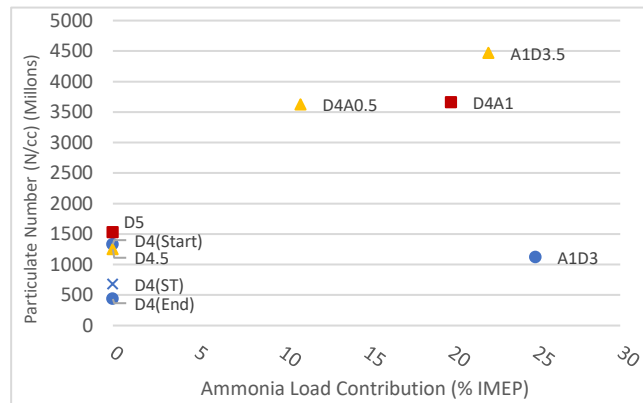


Figure 3.6: Timing of peak in-cylinder temperatures and peak heat release rate detected in tests conducted at various engine loads and ammonia injection rates

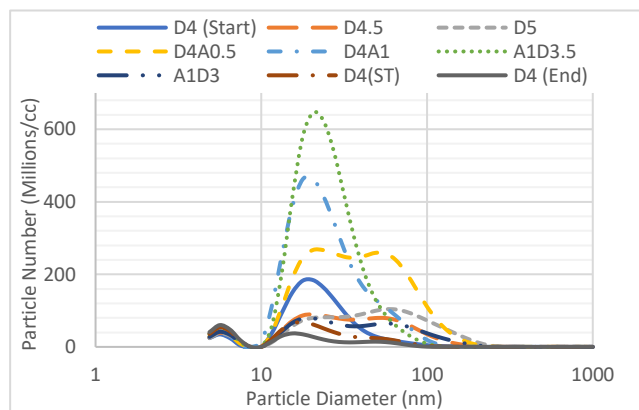
3.5. Particulate emissions



(a)



(b)



(c)

Figure 3.7: Particulate mass (a) and number (b) emissions, and size distribution (c) in the exhaust gases of tests conducted at various engine loads and ammonia injection rates. For (a) and (b), Blue circle (4bar), Yellow triangle (4.5bar), Red square (5bar)

Particulate emissions are not often reported during combustion testing with ammonia. However, Reiter and Kong published further results to their 2008 paper with soot emissions recorded,⁴⁰ observing a decrease in soot concentration as diesel was displaced with ammonia during combustion.

However, they also state that soot emissions are increased if combustion temperatures are too low, with reduced rates of soot oxidation. For instance, 80:20 diesel: ammonia combustion saw higher emissions of soot than 100% diesel, since there was still sufficient carbon within the fuel mix to produce soot, but the lower combustion temperature from the 20% ammonia reduced soot oxidation rates. The particulate mass and number measured during the current study is plotted in Figure 3.7. The first observation is the general increase in particle mass as IMEP increases. This is expected given the increase in the duration of diesel injection and therefore fuel carbon available to undergo pyrolysis and form particulates. Upon aspiration of ammonia to increase the engine load from 4bar- D4(Start)- to 4.5bar IMEP (D4A0.5), the particulate mass and number increased, despite no change in hydrocarbon fuel input. Relatively, the particle number appeared to increase to a greater extent than that of the mass, potentially attributed to the longer ignition delay period, reducing the time subsequently available for particulate agglomeration. With regards to the increase in particle mass, this could be attributed to the increasing proportion of ammonia (and water) within the cylinder and the subsequent dilution of available air, though it was estimated that the reduction of air in the charge gas was slightly less than 4% during peak ammonium hydroxide injection. The same pattern is observed when comparing the tests at equivalent load conditions; the particulate mass increased relative to pure fossil diesel (D4.5 compared to D4A0.5) combustion. The cooling effect of aqueous ammonia aspiration on the air inlet from 80°C (diesel only test) to atmospheric temperature (diesel and ammonia test) could also be a cause for the increased particulate mass, as this may have had a negative impact on fuel vaporisation, resulting in a worsening of fuel droplet atomisation within the fuel spray and therefore more favourable conditions for soot formation in this instance. Figure 3.7 shows that diesel-only combustion, with the intake air temperature reduced to atmospheric temperature (D4(ST)), decreased the particulate number to a greater extent than the addition of ammonia (A1D3) relative to the initial diesel test at 4bar IMEP, D4(Start) (with intake air at 80°C). This suggests that the extended ignition delay resulting from a lower intake air temperature is likely the most influential factor in the observed reduction in particulate number and that, potentially, the aspiration of aqueous ammonia counteracts this to an extent, as indicated by the general increase in particle mass and number.

As seen from the CO emissions (Figure 3.4), the supply of aqueous ammonia becomes detrimental to complete combustion after a rate of aspiration equivalent to 20 % of the engine IMEP. This is also apparent from the particulate output, which requires more stable combustion for formation, compared to CO, to supply the temperatures needed for fuel pyrolysis. Particle mass (and number) initially increase with the addition of ammonia, likely due to combustion remaining efficient and the ammonium solution diluting the oxygen availability, promoting greater fuel pyrolysis. Comparing the tests conducted at 5 bar IMEP, where aspirated aqueous ammonia contributed to 1 bar IMEP of engine load (Figure 3.7.b), the particle number also increases (D4A1 relative to D5), as there is still sufficient combustion stability for particulates to form.

From the particle size distribution shown in Figure 3.7c, a major observation to note is the decrease in particulates formed from the start to the end of the testing day, an expected trend as engine warm-up contributes to more efficient combustion. Furthermore, it is clear that the increase in particle number observed from ammonium hydroxide incorporated combustion is due to the increase in number of smaller particles, which would concur with the theory that delayed combustion, caused by an increase in the ignition delay period and subsequent extension of the premixing duration, results in a reduction in agglomeration mode particles, compared to nucleation mode. It is tentatively postulated that a proportion of the ammonia solution supplied is passing through unreacted, without contribution to energy release, and emitted in the exhaust; droplets of unreacted ammonium solution could be a cause of the increase in particle number (but a more minor effect on particulate mass) seen as ammonia aspiration is increased; ammonium salts are considered PM_{2.5} material.⁴¹ The particle

distribution of A1D3.5 appears to support this hypothesis, with a marked increase in smaller particles. Since the particle spectrometer assumes a constant particle density, if these particles were indeed ammonium hydroxide derived, and therefore of distinctly lower density than that assumed, then this could also explain why the particle mass is lower for this test than that with only 12 % contributed from ammonia to the same engine load (in addition to the fact that the particles measured were smaller). Unburnt hydrocarbons, containing carbonyl groups, can react with ammonia, forming nitrogen-containing organic compounds.⁴¹ Furthermore, if a proportion of ammonium hydroxide is passing into the exhaust, it is suggested that chemical reactions between ammonia and reactive groups on the surface of the particulates are possible. These reactive species could be inorganic material, such as PAHs or, more likely, polar volatile organic compounds (VOCs) containing oxygen.⁴² If these reactive groups are removed from the bulk surface, a decrease in particle size can be expected.

While the shift towards smaller particles is noted from D4A1 to A1D3.5, a further reduction in load to 4 bar IMEP (A1D3) does not continue the trend of greater ammonium hydroxide injection leading to smaller particles that are potentially less dense than the assumed value. However, the reduction in engine load may see different factors dominating and, compared against the D4(ST) test, the particulate output across the whole size range also increases for the A1D3 test. The expected increase in smaller particles may not be prevalent at this engine load where ammonia is making up 25 % of combustion energy contribution, since the lower load conditions result in lower temperatures that are potentially below the threshold required for significant fuel pyrolysis. This test sees the most dilute stoichiometry of diesel carbon to air, and so the fact that the particle number (and mass) increases would concur with the results at 4.5bar and 5bar, where ammonia injection sees an increase in particulate formation, most especially in the nucleation mode.

3.6. Modelling Results

Chemical kinetic modelling was undertaken at conditions equivalent to engine tests D4 (Start), D4A0.5 and D4A1, to further investigate the effect on ignition, of introducing aqueous ammonia vapour into the combustion chamber. A comparison of the in-cylinder pressure measured during tests D4 (Start), D4A0.5 and D4A1 and that produced from modelling of the same experiments can be seen in Figure 2Error! Reference source not found..8.

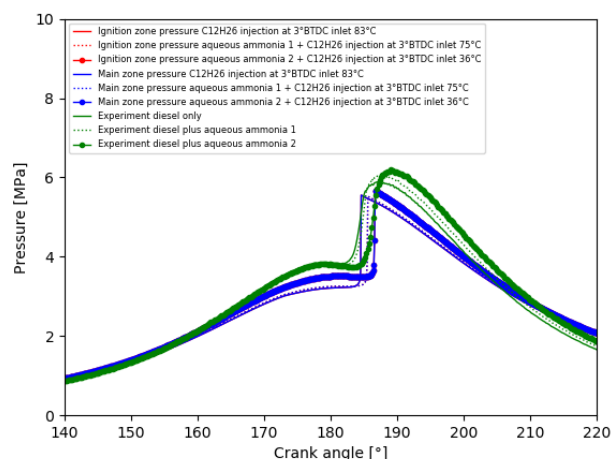


Figure 2.8. In-cylinder pressure measured during tests D4 (Start), D4A0.5 and D4A1 and that produced from chemical kinetic modelling of the same experiment

The experimentally measured in-cylinder pressure shown Figure 2.8 illustrates that as the amount of aqueous ammonia aspirated into the intake air increased, the ignition of the fuel was delayed within the engine cycle (Figure 3.1). At the same time, the inlet temperature into the engine reduced progressively from 83 °C for diesel fuel only (Experiment 1/D4A0.5), to 75 °C (D4A0.5), and eventually to 36 °C (D4A1), for increasing amounts of aqueous ammonia aspirated into the intake air (Table 2.2). The chemical kinetic calculations agreed with the general trend that the addition of aqueous ammonia delayed the ignition of fuel and air in two progressive steps, as the amount of aqueous ammonia was increased, and the inlet temperature was decreased.

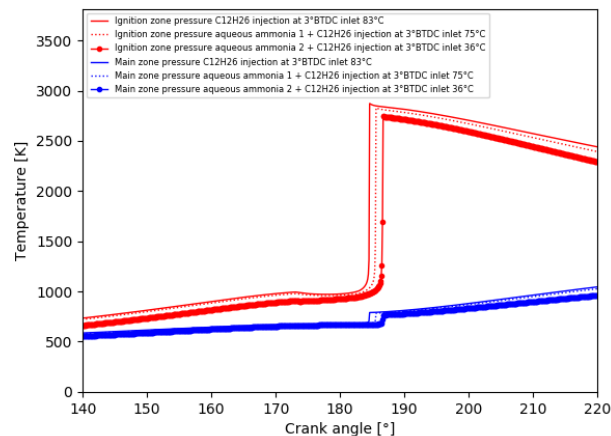


Figure 3.9. Temperature histories modelled for the two reaction zones.

Figure 3.9 shows the temperature histories for the two reaction zones at simulation conditions equivalent to engine experiments D4 (Start), D4A0.5 and D4A1. For all simulations in Zone 1, temperatures reached approximately 1000 K around TDC, just prior to ignition (Figure 3.3). A visible dip in the temperature (Figure 3.9) around the moment of diesel pilot fuel injection represents the reduction in temperature due to the direct injection of diesel fuel (represented by n-dodecane in these simulations) into Zone 1. As ignition of the fuel took place, the temperature within Zone 1 rose rapidly, to approximately 2900K for all three conditions, as the temperature in Zone 1 was dominated by the ignition of diesel fuel taking place under stoichiometric conditions in this zone. Figure 3.9 shows that as the concentration of aspirated aqueous ammonia in the intake was increased, the diesel fuel pilot injection was diluted with a larger amount of aqueous ammonia, in order to maintain stoichiometric conditions. This meant that the total mass of charge enclosed by Zone 1 was increased, which resulted in slightly lower peak temperatures in Zone 1 for those engine operating conditions with higher amounts of aqueous ammonia injected into the intake air. The increased ammonia injection into the intake manifold also reduced the temperature at the start of the compression process and at TDC. This could help in explaining why NO_x emissions and 'global' temperatures calculated from the measured pressure, where one zone was assumed, did not correlate in all cases (Figures 3.5a and 3.5b). Assuming the majority of NO_x was formed in Zone 1, at sufficiently high temperatures, the addition of ammonia and fuel bound nitrogen will likely only increase NO_x until resultant reduction in temperature limits thermal NO_x formation. Furthermore, the ammonia present in Zone 2 is likely not contributing to NO_x as a result of the relatively low temperature, and so any NO_x formed from the fuel itself will be limited by the amount of sufficient (but not over-) mixing of diesel, air and ammonia in Zone 1.

Figure 3.9 also shows that the temperature increase in Zone 2 during ignition was significantly lower than that in Zone 1. This can be attributed to relatively low reaction temperatures in Zone 2, with the main temperature increase in Zone 2 resulting from compression by Zone 1 during ignition, and a moderate amount of heat transfer between the two zones. An important question is whether the homogeneously aspirated ammonia contained in Zone 2 is efficiently oxidised to water and nitrogen during the combustion process, or whether large amounts of unburned fuel risk being emitted along with the exhaust gases, as suggested by the significant increase in particle number with supply of aqueous ammonia equivalent to 1 bar IMEP (Figure 3.7.b).

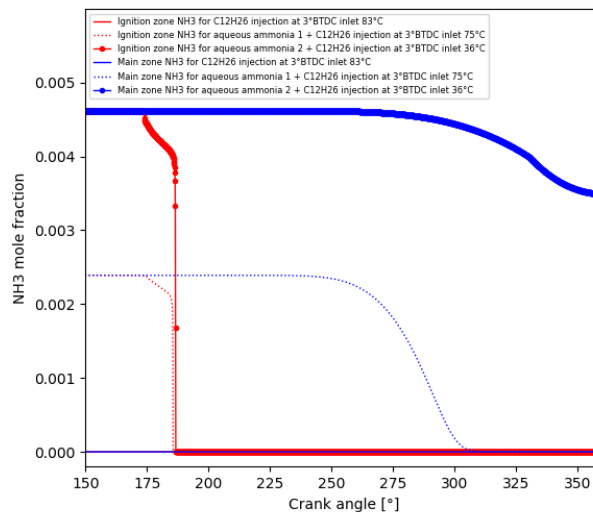


Figure 3.10: Ammonia mole fraction in the reactor zones throughout the engine cycle.

Figure 3.10 shows the ammonia (NH_3) mole fraction in the two engine combustion zones at simulation conditions equivalent to engine experiments D4 (Start), D4A0.5 and D4A1. It can be seen in Figure 3.10 that for each simulation, there is an equivalent concentration of ammonia in both zones until 3 CAD BTDC and diesel fuel injection, confirming the low reactivity of the aspirated aqueous ammonia at these conditions. Following injection of diesel fuel (modelled by $\text{C}_{12}\text{H}_{26}$ in the simulation) into ignition Zone 1, chemical ignition reactions are initiated, leading to some decomposition of the NH_3 . After an initial progressive decomposition, rapid ignition and oxidation of the NH_3 located in Zone 1 takes place for both experiments in which aqueous ammonia was aspirated into the engine (D4A0.5 and D4A1). At first, however, NH_3 concentrations in Zone 2 remain constant and unaffected by the ignition process in Zone 1. At approximately 60 CAD ATDC, heat transfer from Zone 1 to main Zone 2 results in a decrease in NH_3 in the latter through oxidation. In the simulation of D4A0.5, the decomposition of NH_3 in Zone 2 completes just after 300 CAD, while for that of D4A1, the higher initial mole fraction of ammonia, and the lower intake air temperature led to the decomposition of NH_3 remaining incomplete even at 360 CAD, leaving a mole fraction of approximately 3800ppm NH_3 in the exhaust. This highlights the risk of unburned ammonia emissions from engines which have insufficient mixing and heat transfer of the ignition zone with the outer cooler zones, especially when higher concentrations of aqueous ammonia and lower combustion temperatures are used.

In order to filter out the effect which aqueous ammonia has on the ignition process, and to separate it from the effect of the charge cooling caused by the introduction and evaporation of aqueous ammonia into the engine intake, simulations were performed for the same conditions as those described in Figure 3.10 above, but maintaining a constant inlet air temperature of 83° C.

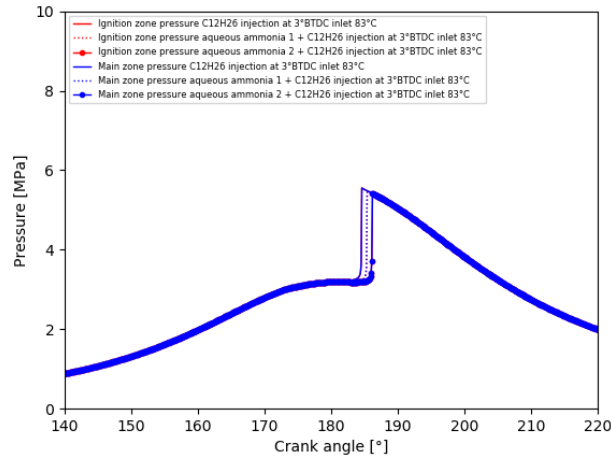


Figure 3.11: In-cylinder pressure from chemical kinetic modelling with increasing engine load contribution from ammonia at constant inlet temperature

Figure 3.11 shows that if the inlet temperature is kept constant, the ignition timing for the pilot ignition of ammonia is quite similar to that when charge cooling from the ammonia was applied (Figure 3.8). This is because the charge-cooling from the ammonia addition was effective in raising the pressure at TDC, due to increased volumetric efficiency of the engine, as apparent in the elevated compression pressures relative to the higher inlet temperature condition in Figure 3.8.

3.7. Modelling potential ways of improving ignition

In order to assess potential ways of improving the ignition characteristics of aqueous ammonia, further simulations were conducted. A potential carbon-free ignition improving additive that could accelerate ignition reactions is aqueous hydrogen peroxide H_2O_2 , which, like 25% aqueous ammonia is liquid under typical atmospheric conditions.

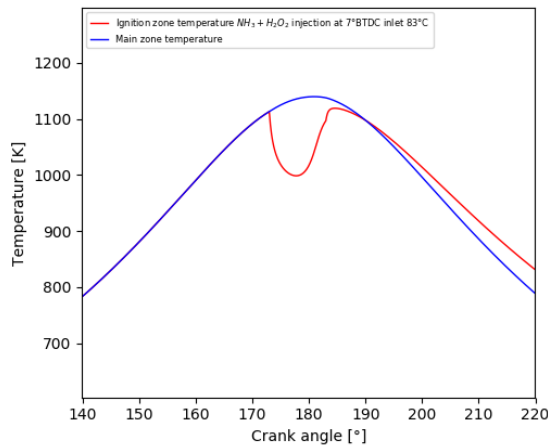


Figure 3.12. Temperature in zones 1 and 2 for ignition of direct injected aqueous ammonia mixed with aqueous hydrogen peroxide.

Figure 3.12 shows that a solution consisting of a mixture of aqueous ammonia and aqueous hydrogen peroxide, yielding molar fractions of 75% H_2O , 20% NH_3 , and 5% H_2O_2 was simulated to just about ignite, even when injected directly into the combustion chamber at 7 degrees BTDC, rather than being aspirated into the intake under the engine conditions simulated in Section 3.6. The simulation

was performed for similar conditions as those used in the engine experiments (Tables 2.1 and 2.2), but using a lower fuel-air equivalence ratio of 0.5. This low fuel-air equivalence ratio was chosen because it did not produce excessive temperature reduction from local charge cooling in zone 1, following injection, but still allowed an observable increase in pressure resulting from ignition (Figure 3.12).

Aqueous hydrogen peroxide therefore shows significant promise for igniting aqueous ammonia, even under direct injection conditions, without the help of another pilot fuel.

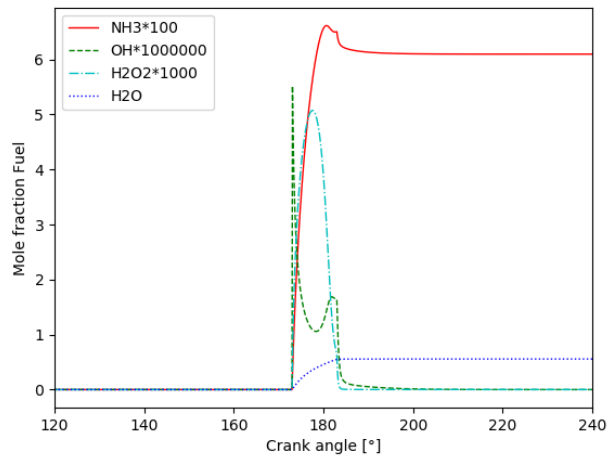


Figure 3.13. Development of intermediate species and final combustion product during ignition of aqueous ammonia with aqueous hydrogen peroxide.

Figure 3.13 shows the development of intermediate species and water as the final combustion product of the combustion of aqueous ammonia and aqueous hydrogen peroxide in the engine. The simulations show that all hydrogen peroxide decomposed during the combustion process, and that the addition of this fuel component was able to promote ignition without the need for an additional pilot injection under these engine conditions. It is also interesting to note the appreciable level of NH_3 persisting beyond the end of combustion at approximately 185 CAD, suggesting a failure of flame propagation beyond local ignition sites at these specific conditions.

4. Conclusions

This study presents experiments utilising intake aspirated aqueous ammonia and direct injection diesel co-combustion in a compression ignition engine, investigating the potential of the ammonia solution to usefully a proportion of the energy provided by diesel fuel and the impact on exhaust emissions of doing so. A two-zone chemical kinetic model of the aqueous ammonia and diesel combustion was also developed, providing insight as to the mechanisms of ammonia ignition at the experimental conditions. From the findings of the engine experiments and modelling presented, the following conclusions can be drawn:

- Ignition of the aspirated aqueous ammonia was achieved, and contributed a maximum of 25% of the total engine load at 4 bar IMEP, albeit resulting in a significantly extended ignition delay period relative to diesel only combustion.

- Exhaust CO emissions increased near linearly with the proportion of engine load provided by aspirated aqueous ammonia, despite a concurrent reduction in the fuel carbon present. A similar increase in engine cycle to cycle variability was also observed, suggesting greater combustion instability with increasing levels of heat release contributed by the premixed aspirated ammonia relative to direct injected diesel.
- Levels of NO_x in the engine exhaust increased initially with the level of aqueous ammonia present, but decreased at ammonia engine load contribution levels greater than 20 %. The initial increase in NO_x may be attributable to the increasing levels of fuel-bound nitrogen present from ammonia, however, at higher levels of aspiration this impact was offset by greater combustion instability and lower temperatures.
- A general increase in both particulate mass and number, as ammonia load contribution was increased, was observed. An especially significant increase in the number of nucleation mode particles was seen as ammonia injection increased, suggestive of the presence of ammonia solution droplets, until the A1D3 test, at which it is suggested diesel was too dilute and combustion temperatures were too low to continue this trend.
- At higher mole fractions of aqueous ammonia aspirated into the intake air, and low intake air temperatures, significant proportions of ammonia were modelled to remain unoxidised in the periphery of the combustion chamber, in agreement with the experimentally observed cycle to cycle variation.
- Modelling of aqueous ammonia mixed with aqueous hydrogen peroxide showed that this mixture could be ignited under the same engine operating conditions even when injected directly into the combustion chamber at 7°BTDC without additional pilot injection.
- This work shows the difficulties involved with ignition of ammonia and ensuring stable combustion, especially in aqueous form and at relatively low engine loads, but also highlights possible pathways for achieving reliable ignition and strategies for avoiding negative impacts on engine exhaust emissions when displacing fossil diesel.

Nomenclature and Units

ATDC = After top-dead centre	ID = Ignition delay (CAD)
BSFC = Brake-specific fuel consumption	IMEP = Indicated mean effective pressure (bar)
BTDC = Before top-dead centre	N ₂ = Nitrogen
CAD = Crank angle degree (°)	NH ₃ = Ammonia
CI = Compression ignition	NH ₄ OH = Ammonium hydroxide
CO = Carbon monoxide	IR = Infrared Radiation
CO ₂ = Carbon dioxide	O ₂ = Oxygen
COV = Coefficient of variation	ppm = Parts per million
DEE = Diethyl ether	NO _x = Nitrous oxides
EGR = Exhaust gas recirculation	pHRR = Peak heat release rate (J/deg)
FAME = Fatty acid methyl ester	PM = Particle mass
H ₂ = Hydrogen	PN = Particle number
H ₂ O = Water	SI = Spark ignition
HCCI = Homogeneous charge compression ignition	SOC = Start of combustion
HRR = Heat release rate (J/degree)	SOI = Start of injection
ICE = Internal combustion engine	ST = Standard temperature
	TDC = Top dead centre

References

1. Zamfirescu, C. & Dincer, I. Ammonia as a green fuel and hydrogen source for vehicular applications. *Fuel Process. Technol.* (2009). doi:10.1016/j.fuproc.2009.02.004
2. Tartakovsky, L. & Sheintuch, M. Fuel reforming in internal combustion engines. *Progress in Energy and Combustion Science* (2018). doi:10.1016/j.pecs.2018.02.003
3. Casanovas, A., Divins, N. J., Rejas, A., Bosch, R. & Llorca, J. Finding a suitable catalyst for on-board ethanol reforming using exhaust heat from an internal combustion engine. *Int. J. Hydrogen Energy* (2017). doi:10.1016/j.ijhydene.2016.11.197
4. Li, H. *et al.* On-board methanol catalytic reforming for hydrogen Production-A review. *International Journal of Hydrogen Energy* (2021). doi:10.1016/j.ijhydene.2021.04.062
5. Woo, S., Baek, S. & Lee, K. On-board LPG reforming system for an LPG · hydrogen mixed combustion engine. *Int. J. Hydrogen Energy* (2020). doi:10.1016/j.ijhydene.2020.02.139
6. Umar, M. *et al.* Hydrogen production from bioethanol fuel mixtures via exhaust heat recovery in diesel engines: A promising route towards more energy efficient road vehicles. *Int. J. Hydrogen Energy* (2021). doi:10.1016/j.ijhydene.2021.04.146
7. Lhuillier, C., Brequigny, P., Contino, F. & Mounaïm-Rousselle, C. Experimental study on ammonia/hydrogen/air combustion in spark ignition engine conditions. *Fuel* (2020). doi:10.1016/j.fuel.2020.117448
8. Reiter, A. J. & Kong, S. C. Demonstration of compression-ignition engine combustion using ammonia in reducing greenhouse gas emissions. *Energy and Fuels* (2008). doi:10.1021/ef800140f
9. Kroch, E. Ammonia - A Fuel for Motor Buses. *J. Inst. Pet.* **31**, 213–223 (1945).
10. Gray, J. T., Dimitroff, E., Meckel, N. T. & Quillian, R. D. Ammonia fuel - Engine compatibility and combustion. in *SAE Technical Papers* (1966). doi:10.4271/660156
11. Duynslaegher, C. & Jeanmart Pr O Gicquel Pr J Martin Pr D Peeters Pr D Puechberty, P. H. *Université catholique de Louvain Experimental and numerical study of ammonia combustion.* (2011).
12. Fenimore, C. P. & Jones, G. W. Oxidation of ammonia in flames. *J. Phys. Chem.* (1961). doi:10.1021/j100820a027
13. Bian, J., Vandooren, J. & Van Tiggelen, P. J. Experimental study of the structure of an ammonia-oxygen flame. *Symp. Combust.* (1988). doi:10.1016/S0082-0784(88)80327-8
14. Frigo, S. & Gentili, R. Analysis of the behaviour of a 4-stroke Si engine fuelled with ammonia and hydrogen. *Int. J. Hydrogen Energy* (2013). doi:10.1016/j.ijhydene.2012.10.114
15. Grannell, S. M., Assanis, D. N., Bohac, S. V. & Gillespie, D. E. The fuel mix limits and efficiency of a stoichiometric, ammonia, and gasoline dual fueled spark ignition engine. *J. Eng. Gas Turbines Power* (2008). doi:10.1115/1.2898837
16. Grannell, S. M., Assanis, D. N., Bohac, S. V. & Gillespie, D. E. The operating features of a stoichiometric, ammonia and gasoline dual fueled spark ignition engine. in *2006 ASME International Mechanical Engineering Congress and Exposition, IMECE2006 - Energy* (2006). doi:10.1115/IMECE2006-13048
17. Grannell, S. M., Assanis, D. N., Gillespie, D. E. & Bohac, S. V. Exhaust emissions from a stoichiometric, ammonia and gasoline dual fueled spark ignition engine. in *Proceedings of the Spring Technical Conference of the ASME Internal Combustion Engine Division* (2009). doi:10.1115/ICES2009-76131
18. Starkman, E. S., Newhall, H. K., Sutton, R., Maguire, T. & Farbar, L. Ammonia as a spark ignition engine fuel: Theory and application. in *SAE Technical Papers* (1966). doi:10.4271/660155
19. Sawyer, R. F., Starkman, E. S., Muzio, L. & Schmidt, W. L. Oxides of nitrogen in the combustion products of an ammonia fueled reciprocating engine. in *SAE Technical Papers* (1968).

- doi:10.4271/680401
20. Tanaka, S., Ayala, F., Keck, J. C. & Heywood, J. B. Two-stage ignition in HCCI combustion and HCCI control by fuels and additives. *Combust. Flame* (2003). doi:10.1016/S0010-2180(02)00457-1
 21. Wang, W., Herreros, J. M., Tsolakis, A. & York, A. P. E. Ammonia as hydrogen carrier for transportation; Investigation of the ammonia exhaust gas fuel reforming. *Int. J. Hydrogen Energy* (2013). doi:10.1016/j.ijhydene.2013.05.144
 22. Comotti, M. & Frigo, S. Hydrogen generation system for ammonia-hydrogen fuelled internal combustion engines. *Int. J. Hydrogen Energy* (2015). doi:10.1016/j.ijhydene.2015.06.080
 23. Westlye, F. R., Ivarsson, A. & Schramm, J. Experimental investigation of nitrogen based emissions from an ammonia fueled SI-engine. *Fuel* (2013). doi:10.1016/j.fuel.2013.03.055
 24. Ryu, K., Zacharakis-Jutz, G. E. & Kong, S. C. Effects of gaseous ammonia direct injection on performance characteristics of a spark-ignition engine. *Appl. Energy* (2014). doi:10.1016/j.apenergy.2013.11.067
 25. Koike, M. *et al.* Cold-start performance of an ammonia-fueled spark ignition engine with an on-board fuel reformer. *Int. J. Hydrogen Energy* (2021). doi:10.1016/j.ijhydene.2021.05.052
 26. Dimitriou, P. & Javaid, R. A review of ammonia as a compression ignition engine fuel. *International Journal of Hydrogen Energy* (2020). doi:10.1016/j.ijhydene.2019.12.209
 27. Pochet, M., Dias, V., Jeanmart, H., Verhelst, S. & Contino, F. Multifuel CHP HCCI Engine towards Flexible Power-to-fuel: Numerical Study of Operating Range. in *Energy Procedia* (2017). doi:10.1016/j.egypro.2017.03.468
 28. Christensen, M., Johansson, B., Amnéus, P. & Mauss, F. Supercharged homogeneous charge compression ignition. in *SAE Technical Papers* (1998). doi:10.4271/980787
 29. Wang, Y., Zhou, X. & Liu, L. Theoretical investigation of the combustion performance of ammonia/hydrogen mixtures on a marine diesel engine. *Int. J. Hydrogen Energy* (2021). doi:10.1016/j.ijhydene.2021.01.233
 30. Boretti, A. Novel dual fuel diesel-ammonia combustion system in advanced TDI engines. *Int. J. Hydrogen Energy* (2017). doi:10.1016/j.ijhydene.2016.11.208
 31. Lamas, M. I. & Rodriguez, C. G. Numerical model to analyze Nox reduction by ammonia injection in diesel-hydrogen engines. *Int. J. Hydrogen Energy* (2017). doi:10.1016/j.ijhydene.2017.08.090
 32. Gill, S. S., Chatha, G. S., Tsolakis, A., Golunski, S. E. & York, A. P. E. Assessing the effects of partially decarbonising a diesel engine by co-fuelling with dissociated ammonia. *Int. J. Hydrogen Energy* (2012). doi:10.1016/j.ijhydene.2011.12.137
 33. Hellier, P., Al-Haj, L., Talibi, M., Purton, S. & Ladommatos, N. Combustion and emissions characterization of terpenes with a view to their biological production in cyanobacteria. *Fuel* (2013). doi:10.1016/j.fuel.2013.04.042
 34. Heywood, J. . *Internal Combustion Engine Fundamentals*. (McGraw-Hill Inc, 1988).
 35. Frassoldati, A., Faravelli, T. & Ranzi, E. Kinetic modeling of the interactions between NO and hydrocarbons at high temperature. *Combust. Flame* (2003). doi:10.1016/S0010-2180(03)00152-4
 36. Goodwin, D. G. CANTERA: An open-source, object-oriented software suite for combustion. in *NSF Workshop on Cyber-based Combustion Science* (2006).
 37. Duraisamy, G., Rangasamy, M. & Nagarajan, G. Effect of EGR and Premixed Mass Percentage on Cycle to Cycle Variation of Methanol/Diesel Dual Fuel RCCI Combustion. in *SAE Technical Papers* (2019). doi:10.4271/2019-26-0090
 38. Saravanan, S., Nagarajan, G., Anand, S. & Sampath, S. Correlation for thermal NOx formation in compression ignition (CI) engine fuelled with diesel and biodiesel. *Energy* (2012). doi:10.1016/j.energy.2012.03.028
 39. Talibi, M., Hellier, P., Balachandran, R. & Ladommatos, N. Effect of hydrogen-diesel fuel co-combustion on exhaust emissions with verification using an in-cylinder gas sampling

- technique. *Int. J. Hydrogen Energy* (2014). doi:10.1016/j.ijhydene.2014.07.039
40. Reiter, A. J. & Kong, S. C. Combustion and emissions characteristics of compression-ignition engine using dual ammonia-diesel fuel. *Fuel* (2011). doi:10.1016/j.fuel.2010.07.055
 41. Zhu, S. *et al.* Modeling reactive ammonia uptake by secondary organic aerosol in CMAQ: Application to the continental US. *Atmos. Chem. Phys.* (2018). doi:10.5194/acp-18-3641-2018
 42. Goss, K. U. & Eisenreich, S. J. Sorption of volatile organic compounds to particles from a combustion source at different temperatures and relative humidities. *Atmos. Environ.* (1997). doi:10.1016/S1352-2310(97)00048-4